

MAGNETIC PROPERTIES OF NANOPOWDER h-BN DOPED WITH Fe AND Fe₃O₄ NANOCLUSTERS

Sh. Makatsaria^{1,2}, Sh. Kekutia³, J. Markhulia³,
V. Mikelashvili³, L. Chkhartishvili^{1,4}, R. Chedia^{4,5}

¹Georgian Technical University
Engineering Physics Department
Tbilisi, Georgia
levanchkhartishvili@gtu.ge

²Official Representatives of Siemens Healthcare Diagnostics
LLC Deltamed Georgia
Tbilisi, Georgia
s.makatsaria@deltamedgeorgia.com

³Georgian Technical University
Vladimer Chavchanidze Institute of Cybernetics
Tbilisi, Georgia
kekuka@yahoo.com
janomarkhulia@gmail.com
vmikelashvili@gtu.ge

⁴Ferdinand Tavadze Metallurgy and Materials Science Institute
Semiconducting and Powder Composite Materials Laboratory
Tbilisi, Georgia

⁵Ivane Javakhishvili Tbilisi State University
Petre Melikishvili Institute of Physical and Organic Chemistry
Tbilisi, Georgia
chediageo@yahoo.com

Accepted 2022 December 1

Abstract

Hexagonal boron nitride h-BN nanopowders doped with magnetic nanoclusters – ferromagnetic iron Fe and / or ferrimagnetic magnetite Fe₃O₄ – obtained by several novel chemical synthesis routes reveal the magnetic properties making useful application of these nanocomposites in BNCT (Boron Neutron Capture Therapy) for external magnetic field controlled delivery of neutron-capturing boron ¹⁰B isotopes in target tumor cells.

1. Introduction

Boron-rich materials are of interest for the BNCT (Boron Neutron Capture Therapy) actively utilized for treatment of some aggressive cancers, where standard chemo- and radiation therapies reveal disadvantages. BNCT is known to be based on the nuclear reaction ¹⁰B(n,α)⁷Li occurring when the non-radioactive ¹⁰B nucleus interacts with an (epi)thermal neutron. It

yields high LET (Linear Energy Transfer) ⁴He (α-particle) and ⁷Li nuclei having short path-lengths in tissues, comparable with cells mean size. To be the BNCT successful, certain critical number of ¹⁰B atoms should be delivered to the tumor: when such boron-containing particles are bombarded with neutrons the targeted cancer cells are burned out by energetic ³He and ⁷Li nuclei almost without damage to the healthy ones.

In clinical practice, the delivery of boron ¹⁰B isotopes, i.e. neutron-absorbing centers, to cancer cells usually is conducted via boron-containing macromolecules characterized by a predominant accumulation in the tumor. The disadvantage of this approach is the insufficient content of boron in macromolecular carriers. Attempts are done to overcome this problem by developing the boron-containing nanosystems. From the literature analysis [1] our primary choice is made for hexagonal boron nitride h-BN based boron ¹⁰B isotope delivery nanocarriers for their: high boron content; good tumor-to-nontumor boron accumulation ratio; good biocompatibility; low toxicity and negligible other side-effects related to their chemical and oxidative stabilities; possibility to overcome the cancer multidrug resistance mechanisms due to tumor progression; and possibility to undergo rapid on-demand degradation under physiological conditions.

But, how one is able to accumulate the boron nitride nanoparticles in tumor cells? To answer this question note that in many cases the functionalized magnetic nanocomposites can successfully serve for the medical treatment tools. To respond this challenge, in mini-review [2] we have proposed the development of h-BN based magnetic nanopowders combining high boron content with possibility to be transported to tumor cells by exposure to an external magnetic field. Preparation of some boron nitride based fine-dispersive nanocomposites for neutron-therapy via chemical synthesis has been considered in [3, 4].

This work aims to investigate magnetization of obtained in this way h-BN nanopowders doped with magnetic nanoclusters in form of metallic iron Fe and / or its ferrimagnetic oxide Fe₃O₄ – magnetite.

2. Material and method

The five series of nanocomposites were formed by intercalation of reduced magnetic phase into the h-BN layered structure or magnetic phase deposition on the h-BN particles.

Their magnetic characteristics were obtained on powder samples using the VSM (Vibrating Sample Magnetometry) method. Namely, magnetic measurements were performed at room temperature by 7300 Series VSM System (Lake Shore Cryotronics Inc., USA) with applied magnetic field ranging from -14 to +14 kG.

3. Magnetic properties

As is known, magnetic properties of ferro- and ferrimagnetic powder materials depend on particles size. Particles of such magnetic material exhibit multidomain state above a critical diameter D_{c1} , while below this size passes into a monodomain state; and below other critical diameter D_{c2} it exhibits the superparamagnetism [5, 6].

Magnetization curve, i.e. magnetization M as a function $M(H)$ of the applied magnetic field H , provides an important information about material magnetic properties, including saturation M_s and remnant M_r magnetizations, as well as coercive force H_c .

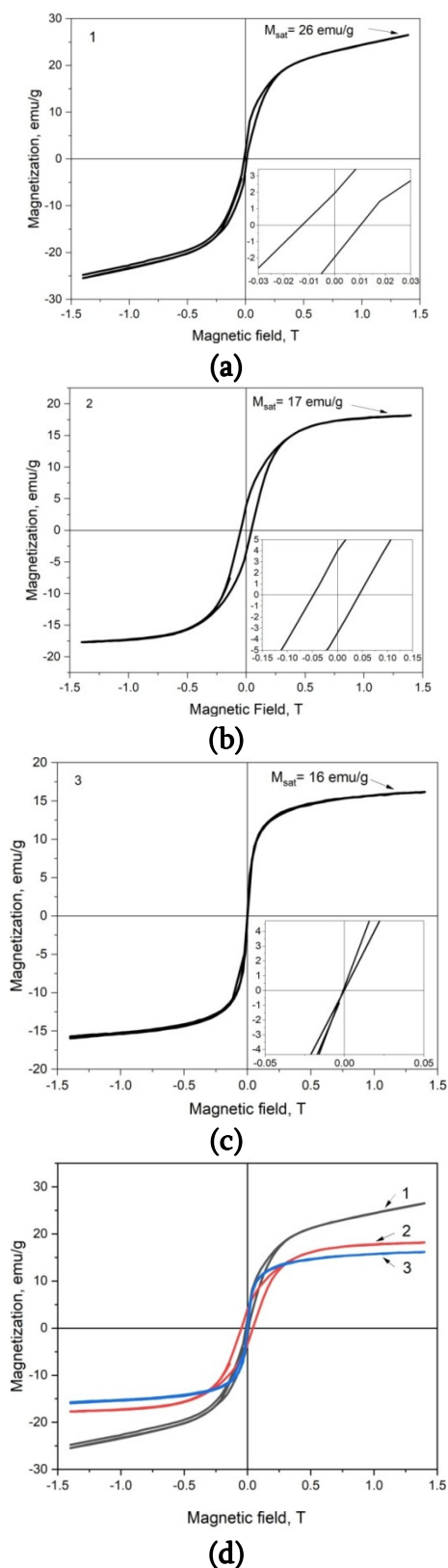
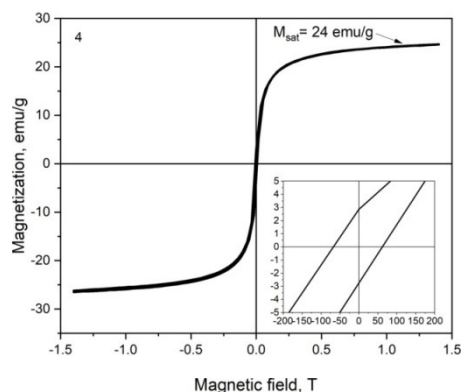


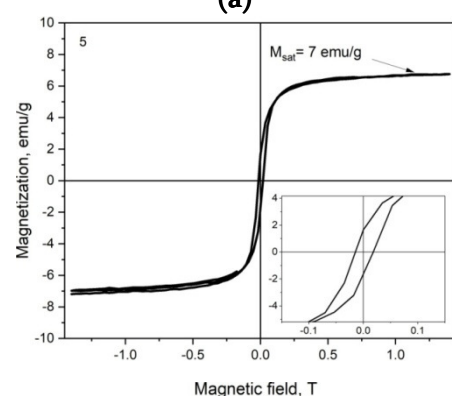
Figure 1. Room temperature magnetization curves for samples (a) 1, (b) 2, (c) 3 and (d) 1, 2 and 3 in comparison.

Figures 1 and 2 present the room temperature magnetization curves and hysteresis loops of synthesized composite samples: 1 – BN–Fe (obtained from FeSO_4 with NaBH_4), 2 – BN–Fe (obtained from BN– Fe_2O_3 with H_2), 3 – BN– Fe_3O_4 (obtained by co-precipitation of Fe^{II} and Fe^{III}

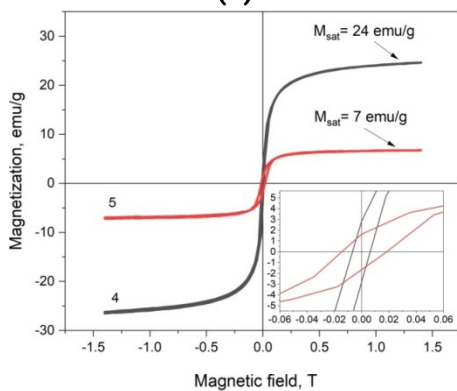
compounds), 4 – BN–Fe (obtained by decomposition of Fe⁰ pentacarbonyl) and 5 – BN–Fe₃O₄ (obtained by decomposition of Fe⁰ pentacarbonyl in presence of H₂O).



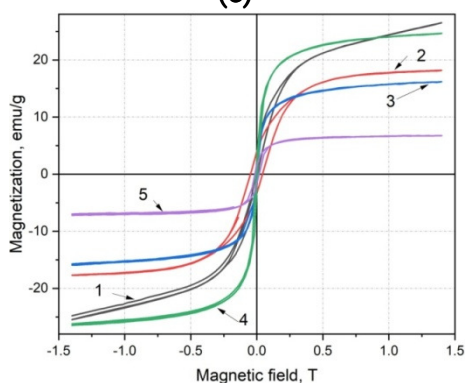
(a)



(b)



(c)



(d)

Figure 2. Room temperature magnetization curves for samples (a) 4, (b) 5, (c) 4 and 5 and (d) 1, 2, 3, 4 and 5 in comparison.

At first sight, one may notice that the magnetization curves (**Figure 1**) of three samples 1, 2 and 5 exhibit hysteresis loops with similar shapes. The magnetization of these samples rises with the increasing magnetic field, initially rapidly up to external field approximately of 5 kG and then gradually. At the maximum applied magnetic field of 14 kG, the magnetizations of these samples were $M_{H_{max}} = 26.5, 18.0$ and 6.75 emu/g, respectively. We should note that here the magnetization of sample 1 is not completely saturated at the maximum value of the applied external magnetic field. As for the sample 2, we can say that its $M_{H_{max}}$ value is very close to the saturation. And for sample 5, the $M_{H_{max}}$ value coincides with M_s . For these three samples M_R and H_c equal to 1.85, 3.80, 1.76 emu/g and 114, 456, 164 G, respectively.

In general, M_s and M_R increase with material crystallinity and the variation of its coercivity can be caused by various combined factors such as atoms distribution in the magnetic phase structure and crystallites size and distribution in the composite [5, 7]. Thus, it is workable to notice that these samples exhibit similar magnetic behavior, characteristic of soft magnetic materials. Among them the sample 1 is closest to the behavior of superparamagnetic material.

The room temperature magnetization curves for samples 3 and 4 are displayed in **Figure 2**. Corresponding magnetization hysteresis loops are S-shaped and extremely thin due to the absence of remnant magnetization and negligible coercivity. More precisely, in sample 3 actually there is no coercivity ($M_{H_{max}} = 16$ emu/g) and, therefore, this nanocomposite exhibits superparamagnetic behavior. As for the sample 4, there is a small coercivity ($H_c = 63$ G and $M_{H_{max}} = 24.5$ emu/g) and in behavior it shows similarities with the sample 1.

4. Conclusion

Iron Fe valent states – Fe^0 , $Fe^{II}Fe_2^{III}O_4$ and $Fe_2^{III}O_3$ – characteristic of free metallic iron Fe, magnetite Fe_3O_4 and maghemite Fe_2O_3 , respectively, lead to ferro-, ferri- and antiferromagnetic properties. Consequently, hexagonal boron nitride h-BN doped with Fe have to be the best magnetic among the studied three composites. But, using h-BN:Fe in BNCT is problematic because of iron fast oxidation in aqueous media. As for the h-BN:Fe₂O₃, it not a magnetic at all. Thus, the magnetite-doped hexagonal boron nitride h-BN:Fe₃O₄ should be considered for an optimal choice.

Acknowledgement

Sh. Makatsaria acknowledges that this research has been supported by Shota Rustaveli National Science Foundation of Georgia (SRNSFG) Doctoral Educational Programs Grant # PHDF–22–1299: “Obtaining and Structural-Morphological Characterization of Nanopowder Boron Compounds Doped with Ferromagnetic Clusters” (2022 – 2023).

References

- [1] Sh. Makatsaria, L. Chkhartishvili, R. Chedia, O. Tsagareishvili. Boron carbide and nitride nanoparticles as ¹⁰B-isotope delivering agents in boron-neutron-capture-therapy. In: Abs. 6th Int. Conf. “Nanotechnology” – GTU nano 2021 (Eds. L. Chkhartishvili, M. Chikhradze), 2021, Tbilisi, Publ. House “Tech. Univ.”, 80-80.

- [2] Sh. Makatsaria, L. Chkhartishvili, Sh. Dekanosidze, R. Chedia. Nanopowder boron compounds doped with ferromagnetic clusters for BNCT. *Int. J. Adv. Nano Comput. Anal.*, 2023, 2, 1, 1-12.
- [3] L. Chkhartishvili, R. Chedia, O. Tsagareishvili, M. Mirzayev, Sh. Makatsaria, N. Gogolidze, N. Barbakadze, M. Buzariashvili, O. Lekashvili, I. Jinikashvili. Preparation of neutron-capturing boron-containing nanosystems. In: *Proc. 9th Int. Conf. Exh. Adv. Nano Mater.*, 2022, Victoria, IAEMM, 1-15.
- [4] L. Chkhartishvili, Sh. Makatsaria, N. Gogolidze. Boron-containing fine-dispersive composites for neutron-therapy and neutron-shielding. In: *Proc. Int. Sci. Prac. Conf. "Innovations and Modern Challenges – 2022"*, 2023, Tbilisi, Publ. House "Tech. Univ.", 221-226.
- [5] J. S. Lee, J. M. Cha, H. Y. Yoon, J. K. Lee, Y. K. Kim. Magnetic multi-granule nanoclusters: A model system that exhibits universal size effect of magnetic coercivity. *Sci. Rep.*, 2015, 5, 12135, 1-7.
- [6] C. Binns. Ch. 1: Tutorial Section on Nanomagnetism. *Front. Nanosci.*, 2014, 6, 1-32.
- [7] T. G. Avancini, M. T. Souza, A. P. N. de Oliveira, S. Arcaro, A. K. Alves. Magnetic properties of magnetite-based nano-glass-ceramics obtained from a Fe-rich scale and borosilicate glass wastes. *Ceram. Int.*, 2019, 45, 4, 4360-4367.